Performance Characterization of Spatially Random Energy Harvesting Underlay D2D Networks with Primary User Power Control

S. Kusaladharma and C. Tellambura, *Fellow*, *IEEE*
Department of Electrical and Computer Engineering
University of Alberta, Edmonton, Alberta T6G 2V4, Canada
Email: kusaladh@ualberta.ca and chintha@ece.ualberta.ca

***Abstract*—Energy harvesting underlay device-to-device (D2D) networks are a promising solution to increase spectral and energy efficiency of wireless systems. However, to what extent is the performance of such networks affected by spatial randomness, temporal correlations, power control procedures, and channel uncertainties? To answer this question, we consider an environment with a multi channel primary user network whose nodes and D2D transmitters are spatially distributed as a homogeneous Poisson point process and the wireless signals are subject to log-distance path loss, Rayleigh fading, and path loss inversion based power control. We derive expressions for the ambient radio frequency power available for harvesting at a D2D transmitter, and approximate it using a Gamma distribution. Furthermore, we use a Markov chain model to derive the probability of a successful energy harvest for single slot and multi slot harvesting schemes, and derive the coverage performance of a D2D receiver when a D2D transmitter gets assigned to a sub-band randomly. It is concluded that a D2D receiver sensitivity between -120 dBm and -100 dBm is optimum for both single and multi-slot harvests, and that a higher primary transmitter density is detrimental to multi slot harvesting when the D2D transmitter-receiver distance increases.**

I. Introduction

While wireless communications has experienced a significant growth in recent decades, its continued growth has been hampered by spectral and energy efficiency constraints [1]. An attractive solution to increase spectral efficiency is the use of underlay cognitive radio (CR) networks which allow simultaneous spectrum access for licensed primary users (PUs) and opportunistic secondary users in an interference tolerant basis. This underlay paradigm is ideal for conducting device-to-device (D2D) communications, where two nearby devices directly communicate with each other without the intervention of a central base station [2]. However, D2D transmissions may cause interference to the primary network, and hence exclusion regions and transmit power constraints are enforced which may hinder the D2D network throughput.

Moreover, D2D nodes may use energy harvesting to improve their energy efficiency. While initial attention was directed towards extracting energy from natural sources, harvesting radio frequency (RF) energy has received heightened attention [3]. Although the capabilities of current harvesting circuitry is still limited, because underlaid D2D networks have low power requirements, energy harvesting from the overlaying PU network is an attractive solution. However, the spatial randomness of energy sources and D2D devices, transmit power variations due to power control schemes, and wireless channel uncertainties are significant challenges to a successful energy harvest, and as a result, the amount of energy harvested becomes stochastic in nature [4], [5]. Thus, our focus in this paper is to study the performance of a spatially random energy harvesting D2D network underlaid on a multi-channel cellular network employing power control.

A. Related Work

The performance of energy harvesting networks has received heightened research attention lately. A D2D network underlaying a cellular network is modeled and analyzed in [2] where the D2D transmitters harvest energy from ambient interference. The authors show that energy harvesting can be a reliable alternative to power D2D devices while ensuring acceptable performance. Reference [6] analyzes a set of random primary and secondary devices which communicate with their receivers located a fixed distance away, and derives the optimal transmit power and secondary user density to achieve maximum throughput. Moreover, a novel energy field model is introduced in [7] and the network coverage of a cellular network powered by energy harvesting is characterized, while a tractable K-tier heterogeneous model with energy harvesting base stations is introduced in [8]. In addition, [9], [10] propose dynamic spectrum and power allocation schemes for energy harvesting underlaid D2D networks.

B. Motivation and Contribution

In this paper, we derive the performance of a underlaid D2D device which harvests energy from an overlaying multi-channel PU network. The performance is dependent on the energy harvesting success and the aggregate interference, which are not complimentary conditions. Higher ambient energy ensuring a successful energy harvest may also mean additional interference which hinder the D2D links. The spatial randomness of D2D nodes and primary nodes makes the harvested energy levels random and unreliable, and affects the aggregate interference. Furthermore, this process is also affected by power control procedures and channel uncertainties. Moreover, when a D2D receiver is unable to harvest energy within a single harvesting period, temporal dynamics must be considered.

To analyze how all these factors affect the aggregate interference is our goal. To this end, we model PU devices (transmitters and receivers) and D2D transmitters as three independent homogeneous Poisson point processes in $\mathbb{R}^2$, where PU receivers associate with their closest PU transmitters and each D2D transmitter is associated with a corresponding receiver randomly distributed within a given distance from it. Log distance path loss and Rayleigh fading are assumed. Each PU transmitter uses multiple frequency sub-bands to communicate with receivers and uses path loss inversion based power control. Furthermore, an exclusion region without D2D transmissions is enforced around every PU receiver. The D2D transmitters harvest ambient RF energy from the PU system and transmit their data within a single sub-band. Our contributions can be summarized as follows:

1) By using stochastic geometry, we derive the moment generating function (MGF), the mean, and the variance of the aggregate ambient RF power at a D2D transmitter, and approximate the distribution of the aggregate interference with a Gamma distribution using moment matching. Moreover, the probability of a PU transmitter using a particular sub-band is derived for random sub-band assignment
2) We derive the probability of a successful energy harvest considering temporal correlation for two harvesting schemes using Markov chains. First, a single time slot harvest scheme is considered where transmissions occur irrespective of the harvested energy. Second, a multi slot harvest scheme is considered where a D2D transmitter waits till the harvested energy satisfies transmission requirements.
3) We characterize the coverage performance of a D2D link for a channel assignment protocol where each D2D transmitter selects a random sub-band.

Notations: $\Gamma(x,a) = \int_a^\infty t^{x-1}e^{-t}dt$ and $\Gamma(x) = \Gamma(x,0)$. $\Pr[A]$ is the probability of event A, $f_X(\cdot)$ is the probability density function (PDF), $F_X(\cdot)$ is the cumulative distribution function (CDF), $M_X(\cdot)$ is the MGF, and $E_X[\cdot]$ denotes the expectation over random variable X.

II. System Model

This section introduces the spatial distribution of primary and D2D nodes, the wireless channel model, receiver selection schemes, and power control procedures.

A. Spatial Distribution

The network is broadly divided into primary and D2D nodes. We assume that both these networks are co-located but separate. In other words, we assume that primary receivers do switch to be a D2D node and vice-versa.

1) Primary Network Distribution: The primary network is divided between PU transmitters (base stations) and PU receivers (users), which are distributed in $\mathbb{R}^2$. Base station locations have traditionally been pre-planned, leading to the common assumption of a hexagonal grid with base stations at the centers. However, with the advent of heterogeneous cells such as femtocells and picocells, the base station locations and numbers have been increasingly irregular and random. Therefore, spatial randomness is most appropriate to model current mobile base stations. To this end, the Poisson point process has been extremely popular to model wireless network nodes [11]–[13]. In addition to the analytical tractability, this model has been shown to accurately approximate planned network set-ups [14].

In this paper, we will thus use a homogeneous Poisson point process to model the PU transmitters, where the intensity of the process (average node density) does not depend on the spatial co-ordinates. While non-homogeneous distributions may perhaps suit actual real world scenarios, we will not consider non-homogeneity in order to develop a more general analysis. In a homogeneous Poisson point process with intensity λ, the number of nodes (n) within an enclosed area $\mathcal{A}$ is Poisson distributed [15] with

$$\Pr[N(\mathcal{A}) = n] = \frac{(\lambda\mathcal{A})^n}{n!}e^{-\lambda\mathcal{A}}. \tag{1}$$

As such, we model the PU transmitters with the process Φ_{pt} with intensity $\lambda_{pt}(>0)$. Similarly the primary receivers are also modeled as a homogeneous Poisson point process Φ_{pr} with intensity $\lambda_{pr}(>0)$. Furthermore, since a base station typically serves multiple receivers, we further assume that $\lambda_{pt} < \lambda_{pr}$. Moreover, it is assumed that Φ_{pt} and Φ_{pr} are stationary, and independent of each other. All of these assumptions are common in the literature.

2) D2D Network Distribution: The D2D network consists of transmitter and receiver pairs, and are distributed in $\mathbb{R}^2$. We again employ the homogeneous Poisson point process to model the D2D transmitters as Φ_{d2d} with intensity $\lambda_{d2d}(>0)$. The D2D receivers are modelled to be distributed uniformly surrounding each D2D transmitter within an annular area having a radius of d_l. Without the loss of generality, each D2D transmitter is assumed to be paired with a unique receiver. However, in practice, there may be occasions where a D2D transmitter may not have an associated receiver. In such occasions, the Colouring Theorem [15] shows that the D2D transmitters having an associated receiver follows a thinned homogeneous Poisson process. If the intensity of this thinned process is $\hat{\lambda}_{d2d}$, it can be expressed as $\hat{\lambda}_{d2d} = \kappa\lambda_{d2d}$, where κ is the probability that a D2D transmitter has an associated receiver[1]

B. Channel Model

The primary network employs universal frequency reuse. The frequency band which is used for the downlink is divided into K sub-bands where each can accommodate a different PU receiver. The wireless signals undergo power-law path loss and small scale fading. The path attenuation is assumed to follow the simplified path loss model of [16] where the received

[1]This same D2D spatial model can be alternately expressed as follows. The D2D transmitters and receivers form separate independent Poisson point processes, and each transmitter randomly selects a receiver within a distance d_l, where a receiver can be connected to multiple transmitters concurrently.

power P_R at a distance r from the transmitter emitting signals with a power of P_T is written as $P_R = P_T r^{-\alpha}$, where α is the path loss exponent ranging between $2-6$ [17]. The value of α is assumed to be constant within the k sub-bands. However, this path loss model does not hold whenever $r \to 0$ as the received power $P_R \to \infty$. Therefore, as a workaround, we can take the path loss to be unity whenever $0 < r < 1$, and $P_R = P_T$. Due to the probability of receivers falling within 1m of the transmitter being extremely small, this alteration does not significantly affect the overall statistics, and these two path loss models can be used interchangeably.

The small-scale fading follows the Rayleigh fading model. Consequently, the channel power gain $|h|^2$ is exponentially distributed with $f_{|h|^2}(x) = e^{-x}, 0 < x < \infty$. The fading gains of different links are uncorrelated.

C. Power Control and Transmitter-receiver Association

Both primary and D2D transmitters employ a power control scheme which inverts the path loss in order to ensure a fixed received power level on average which will be the receiver sensitivity[2]. If the receiver sensitivities of the primary and D2D receivers are respectively ρ_p and ρ_{d2d}, the transmit power when the receiver is at a distance r can be written as $P_T = \rho_* r^\alpha$, where $* \in \{p, d2d\}$ [18]. Although path loss inversion based power control scheme is potentially subject to excessive transmit power requirements, this difficulty is alleviated in our system model because PU transmitters are base stations connected to a continuous power supply. Moreover, for the D2D transmitters, the assumption that the receiver is within a radius of d_l naturally incorporates peak-power constraints, as the maximum possible transmit power requirement is $\rho_{d2d} d_l^\alpha$.

For the primary network, the PU receivers associate with the PU transmitter closest to it. This closest transmitter may be determined using GPS information, databases containing locations, or using periodic fixed-power pilot sequences. In the latter case, the closest receiver would provide the best received power on average. We hasten to add that another transmitter may still provide better instantaneous received power levels. With such an association policy, the spatial area would get divided into Voronoii cells surrounding each PU transmitter. In other words, PU receivers within a particular Voronoii cell would associate with the cell's PU transmitter. We assume that out-of-cell associations do not take place. The distance between a PU receiver and its associated transmitter can be found using the void probability of a Poisson point process, and follows the Rayleigh distribution with

$$f_X(x) = 2\pi\lambda_{pt} x e^{-\pi\lambda_{pt}x^2}, 0 < x < \infty. \quad (2)$$

Without any loss of generality, we assume that all PU receivers require a connection with a PU transmitter, and that no receiver is idle unless all the sub-bands of the transmitter are occupied. The Colouring theorem can be easily employed if only a subset of the PU receivers need to be serviced at any given time.

[2]Note that the instantaneous received power may still vary depending on small scale fading

For the D2D network, the association rule is simple where each transmitter connects with its paired receiver. The transmitter-receiver distance in this case follows a linear distribution with

$$f_X(x) = \frac{2x}{d_l^2}, 0 < x < d_l. \quad (3)$$

Similar to the primary network, without loss of generality, each D2D transmitter has data to be disseminated at any given time instant.

Because D2D users are underlaid upon the existing primary network, guard regions must be employed [19]. Guard regions are areas around the primary users within which D2D users are barred from transmitting, and helps to keep the PU interference in-check. D2D users learn about the guard region either through a central database or dynamically through periodic control sequences from the primary users. As such, we consider guard regions around PU receivers. While employing guard regions around PU transmitters is also possible, it is more appropriate to have them surrounding PU receivers in order to better protect them from interference; a PU receiver outside a PU transmitter's guard region or close to the edge may face harmful interference. Moreover, as the D2D transmitters harvest energy from PU transmitters, guard regions around PU transmitters effectively bar D2D users with the best potential of harvesting energy from transmitting.

The guard regions are assumed to be annular regions with a radius of d_g. Let Φ_{pr} be denoted by the set of points $\{x_1, x_2, ...\}$, and $\phi_{pr,i}$ be the primary receiver located at x_i where $i \in \Phi_{pr}$. The guard region encircling $\phi_{pr,i}$ is thus denoted as $b(x_i, d_g)$. Therefore, if Φ_{d2d} is represented by $\{y_1, y_2, ...\}$, and $\phi_{d2d,j}$ is the j-th D2D transmitter located at y_j ($j \in \Phi_{d2d}$), it is precluded from transmitting if $y_j \in \mathcal{A}_\mathcal{G}$. Here, $\mathcal{A}_\mathcal{G} \in \mathbb{R}^2$ is the area of all the guard regions given by $\mathcal{A}_\mathcal{G} = \bigcup_{i \in \Phi_{pr}} b(x_i, d_g)$. Now, let the process of D2D transmitters outside $\mathcal{A}_\mathcal{G}$ be denoted as $\tilde{\Phi}_{d2d}$. $\tilde{\Phi}_{d2d}$ is non-homogeneous, and forms what is termed a Poisson hole process. Let ν be the probability that $\phi_{d2d,j}$ lies outside $\mathcal{A}_\mathcal{G}$, and alternatively is the probability that no PU receiver falls within a distance d_g from $\phi_{d2d,j}$. We can thus obtain ν from (1) as $\nu = e^{-\pi\lambda_{pr} d_g^2}$.

D. D2D Network Operation

The D2D transmitters rely on ambient RF energy harvesting from the primary network to power their circuits. We assume that the power conversion circuits have an efficiency of $\beta(< 1)$, and that energy is harvested in the downlink phase from all sub-bands. Let a PU downlink time slot have length T. If the D2D transmitter requires additional energy at the beginning of a time slot, it will allocate the entire time slot for energy harvesting. Therefore, even in the best case scenario when the required energy is harvested in each time slot, data transfer is performed only on 50% of the time slots.

One weakness of energy harvesting D2D networks is the inherent unreliability. The harvested energy may not be enough to transmit ensuring the receiver sensitivity is met. We thus

consider two schemes. In the first scheme, the D2D transmitter conducts the data transmission irrespective of the harvested energy level. Such a scheme is most appropriate when the D2D users have time critical data to transfer. In the second scheme, the D2D transmitter waits multiple time slots till the harvested energy is greater than the required transmission energy. Under both schemes, full power depletion occurs, and the D2D transmitter returns to a 0 power state after transmission.

The D2D transmitters use a single sub-band within the k different sub-bands for their transmissions. The selection of the sub-band has significant implications on the resultant interference to both the PU and D2D receivers. To this end, we will consider two protocols: 1) each D2D randomly selects a sub-band, and 2) all D2D transmitters use a particular sub-band which has the lowest priority for usage by the PU system. The first protocol has the advantage of lower intra-D2D interference, while the second protocol lowers inter-network interference when the number of PU receivers within a cell falls below K. However, the second protocol has disadvantages of high intra-D2D interference and high interference for the PU receiver using the q-th sub-band. Moreover, in order for the second protocol to work, the D2D users must know in advance which sub-band will be used the last.

III. Energy Harvesting

The D2D network operates by harvesting ambient RF energy to power their transmissions. In this section, we will derive expressions for the total harvested energy, and the probability of a successful energy harvest within the harvesting period.

Let P be the received ambient RF power (then βPT becomes the harvested energy) at the j-th D2D transmitter $\phi_{d2d,j}$, which we can consider to be at the origin without the loss of generality. P is composed of transmitted signals from all PU transmitters, and we can write $P = \sum_{l\in\Phi_{pt}} P_l$, where P_l is the ambient RF power from the l-th PU transmitter $\phi_{pt,l}$. P_l is written as $P_l = \sum_{k=1}^{K} C_{k,l}\rho_p \hat{r}_{k,l}^{\alpha}|h_l|^2 g(r_l)$, where the term $\rho_p \hat{r}_{k,l}^{\alpha}$ is the transmit power from $\phi_{pt,l}$ to the PU receiver using the k-th sub-band located at a distance of $\hat{r}_{k,l}$ from it. $|h_l|^2$ and $g(r_l) = \min(1, r_l^{-\alpha})$ are respectively the small-scale channel power gain and the path loss between $\phi_{pt,l}$ and $\phi_{d2d,j}$, and $C_{k,l}$ is the probability that the k-th sub-band is in occupation during the specific harvesting time-slot.

In order conduct further analysis with P, we will evaluate the MGF of it, which is defined as $M_P(s) = \mathbb{E}[e^{-sP}]$. Using the Campbell's Theorem [15], we can write $M_P(s)$ as

$$M_P(s) = e^{\int_0^{\infty} \mathbb{E}\left[e^{-s\sum_{k=1}^{K} C_{k,l}\rho_p \hat{r}_{k,l}^{\alpha}|h_l|^2 g(r_l)}-1\right] 2\pi\lambda_{pt} r_l dr_l}. \quad (4)$$

Using the fact that $\frac{1}{1+x} = \sum_{v=0}^{\infty}(-x)^v$, and averaging with respect to $|h_l|^2$ and r_l we can simplify $M_P(s)$ as

$$M_P(s) = e^{\left(\sum_{v=1}^{\infty} \frac{\pi\lambda_{pt}\alpha v}{\alpha v-2}(-sC_{k,l}\rho_p)^v \mathbb{E}[(\sum_{k=1}^{K}\hat{r}_{k,l}^{\alpha})^v]\right)}. \quad (5)$$

Because P and its MGF are of complicated forms, it is more advantageous to approximate P with a well known distribution. It has been shown that the received power from a random field of base stations follows a skewed α-stable sistribution which can be closely modelled by the Gamma distribution [20]. The approximation can be accomplished using moment matching where the corresponding moments of P are matched with those of the Gamma distribution. To this end, the MGF can be used to derive the moments of P, where the n-th moment is given by $\mathbb{E}[P^n] = (-1)^n \left[\frac{d^n}{ds^n} M_P(s)\right]_{s=0}$. Therefore, we can find $\mathbb{E}[P]$ and $\mathbb{VAR}[P]$ when $\alpha > 2$ as follows.

$$\mathbb{E}[P] = \frac{\Gamma\left(\frac{\alpha}{2}+1\right)\alpha K C_{k,l}\rho_p}{(\pi\lambda_{pt})^{\frac{\alpha}{2}-1}(\alpha-2)}. \quad (6)$$

$$\mathbb{VAR}[P] = \frac{\alpha(C_{k,l}\rho_p)^2 K}{(\pi\lambda_{pt})^{\alpha-1}(\alpha-1)}\left(\Gamma(\alpha+1) - \left(\Gamma\left(\frac{\alpha}{2}+1\right)\right)^2(1-K)\right) \quad (7)$$

The resultant Gamma distribution can be specified based on its shape and scale parameters k_P and θ_P respectively. Via moment matching, these parameters are obtained as $k_P = \frac{(\mathbb{E}[P])^2}{\mathbb{VAR}[P]}$ and $\theta_P = \frac{\mathbb{VAR}[P]}{\mathbb{E}[P]}$.

A. Deriving $C_{k,l}$

All K sub-bands used by the PU transmitter $\phi_{pt,l}$ have equal probabilities to be assigned for communication with a PU receiver, and thus $C_{k,l}$ remains constant $\forall k \in \{1, 2, ..., K\}$. From intuition, $C_{k,l}$ depends on the number of PU receivers associated with $\phi_{pt,l}$, which is itself dependent on the area of its Voronoii cell. However, the area of a Voronoii cell has no exact distribution. But, an accurate approximation can be made using the Gamma distribution [21]. If $\mathcal{B}$ and $\bar{\mathcal{B}}$ are the cell area and average cell area, the normalized area $\tilde{\mathcal{B}} = \frac{\mathcal{B}}{\bar{\mathcal{B}}}$ of a Voronoii cell is given by $f_{\tilde{\mathcal{B}}}(x) = \frac{\beta_v^{\mu_v}}{\Gamma(\mu_v)} x^{\mu_v-1} e^{-\beta_v x}$, where $\beta_v = 3.57$, $\mu_v = 3.61$, and $\bar{\mathcal{B}} = \frac{1}{\lambda_{pt}}$.

If the number of PU receivers associated with $\phi_{pt,l}$ is Z, $C_{k,l}$ can be expressed as

$$C_{k,l}\backslash z = \Pr[Z \geq K] + \sum_{z=1}^{K-1} \Pr[Z = z]\frac{z}{K}. \quad (8)$$

Using (1) for a given area $\mathcal{B}$ and subsequent averaging by the distribution of $f_{\tilde{\mathcal{B}}}(x)$ results in

$$C_{k,l} = \frac{\beta_v^{\mu_v}}{\Gamma(\mu_v)}\left(\sum_{z=K}^{\infty}\frac{\Gamma(\mu_v+z)\eta^z}{z!(\beta_v+\eta)^{\mu_v+z}} + \sum_{z=1}^{K-1}\frac{\Gamma(\mu_v+z)\eta^z}{K(z-1)!(\beta_v+\eta)^{\mu_v+z}}\right) \quad (9)$$

where $\eta = \frac{\lambda_{pr}}{\lambda_{pt}}$.

IV. D2D Transmission Probability

In this section, we derive the transmission probability of a D2D transmitter for two energy harvesting schemes. For both schemes, we assume that the energy level drops to 0 after a transmission.

A. Single slot harvest

In this scheme, each D2D transmitter attempts a transmission irrespective of the harvested energy in the subsequent time slot. Such a scheme is useful when there is time critical data to be transmitted. Let the distance between the j-th D2D transmitter $\phi_{d2d,j}$ and its receiver be denoted as r_{d2d} with the distribution (3). If the harvested energy $\beta P > \rho_{d2d} r_{d2d}^{\alpha}$,

the transmitted power $P_j = \rho_{d2d} r_{d2d}^{\alpha}$. However, whenever $\beta P < \rho_{d2d} r_{d2d}^{\alpha}$, $P_j = \beta P$. Therefore, $\tau = \Pr[P_j = \beta P]$ can be obtained as

$$\tau = \Pr\left[P < \frac{\rho_{d2d} r_{d2d}^{\alpha}}{\beta}\right] = \int_0^{d_l} \frac{2x}{d_l^2 \Gamma(k_P)} \gamma\left(k_P, \frac{\rho_{d2d} x^{\alpha}}{\beta \theta_P}\right) dx. \quad (10)$$

Let p^{ss} be the probability that $\phi_{d2d,j}$ is ready to transmit at the start of a time slot at steady state. Due to the temporal effects, we use a Markov chain for the analysis. There will be two states within the Markov chain; charged (state 1) and uncharged (state 0). While $\phi_{d2d,j}$ always transitions from the uncharged state to the charged state at the start of the next time slot, it only transitions from the charged state to the uncharged state if it lies outside the guard region $\mathcal{A}_{\mathcal{G}}$. If the state transition matrix is Q, we can write Q as

$$Q = \begin{bmatrix} 0 & 1 \\ \nu & 1-\nu \end{bmatrix}.$$

Let $\Omega = [\omega_0 \ \ \omega_1]$ be the vector comprising steady state probabilities of Q. During steady state, $\Omega = Q\Omega$, and we can derive $p^{ss} = \omega_1 = \frac{1}{1+\nu}$. Thus, the probability of conducting a transmission at the start of a time slot is νp^{ss}.

B. Multi-slot harvest

For this scheme, a D2D transmitter harvests energy in multiple time slots until the total harvested energy βPT is greater than the maximum energy required to transmit, which is $\rho_{d2d} d_l^{\alpha} T$. The main advantage of this scheme is that the D2D transmitter has enough power to ensure that receiver sensitivity requirements are met. However, on the down side, such a scheme is not appropriate for real-time data transfer.

While the harvested energy at the end of a time slot does not confine to discrete levels, for mathematical convenience, we divide the energy levels into $M+1$ discrete states where M can be increased arbitrarily to better reflect the non-discrete nature of the energy level. The 0-th and M-th states respectively denotes the uncharged and fully charged levels. Let the power level of the δ-th state ($0 < \delta < M$) be denoted as E_δ. If $\phi_{d2d,j}$ was initially in state 0, it would transition to state δ whenever $E_\delta \leq \beta PT < E_{\delta+1}$, remain at state 0 if $\beta PT < E_1$, and reach state M if $\beta PT \geq E_M$. Similarly, whenever $\phi_{d2d,j}$ is initially at state δ, the transitioned state increases correspondingly.

The state transition diagram for this scheme is illustrated in Fig. 1, and the state transition matrix Q (with the vector of steady state probabilities being $\Omega = [\omega_0 \ \omega_1 \ . \ . \ \omega_M]$) is expressed as follows.

$$Q = \begin{bmatrix} p_0 & p_1 & p_2 & . & p_{M-1} & 1-\sum_{g=0}^{M-1} p_g \\ 0 & p_0 & p_1 & . & p_{M-2} & 1-\sum_{g=0}^{M-2} p_g \\ 0 & 0 & p_0 & . & p_{M-3} & 1-\sum_{g=0}^{M-3} p_g \\ . & . & . & . & . & . \\ 0 & 0 & 0 & . & p_0 & 1-p_0 \\ \nu & 0 & 0 & . & 0 & 1-\nu \end{bmatrix}.$$

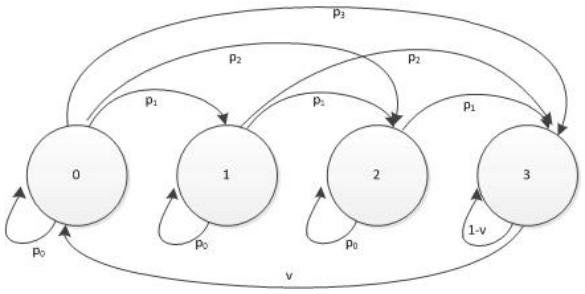

Fig. 1: Markov chain model for multi-slot harvesting with $M = 3$.

Here $p_g (g \in \{1, 2, 3, ..., M-1\})$ refers to the probability of transitioning g states higher from the initial state, and can be expressed as

$$p_g = \Pr\left[\frac{g\rho_{d2d} d_l^{\alpha}}{\beta M} \leq P < \frac{(g+1)\rho_{d2d} d_l^{\alpha}}{\beta M}\right] = \frac{1}{\Gamma(k_P)}\left(\gamma\left(k_P, \frac{(g+1)\rho_{d2d} d_l^{\alpha}}{\beta M \theta_P}\right) - \gamma\left(k_P, \frac{g\rho_{d2d} d_l^{\alpha}}{\beta M \theta_P}\right)\right) \quad (11)$$

Let p^{ms} be the probability that $\phi_{d2d,j}$ is ready to transmit at the start of a time slot, which is also the steady state probability of being at state M. We can obtain p^M as

$$p^{ms} = \omega_M = \frac{1}{1 + \sum_{g=0}^{M-1} \mathcal{D}_g}. \quad (12)$$

Here, $\mathcal{D}_0 = \frac{-\nu}{p_0 - 1}$, and $\mathcal{D}_g = \frac{-1}{p_0 - 1}(\sum_{h=0}^{g-1} p_{g-h} \mathcal{D}_h)$ for $1 \leq g \leq M-1$. It can be easily seen that (12) reduces to p^{ss} when $M = 1$ and $p_0 = 0$. The probability of conducting a transmission at the start of any time slot is thus νp^{ms}.

V. D2D Receiver Performance

Here we analyze the coverage performance of a D2D receiver where each D2D transmitter randomly selects a sub-band $k (k \in \{1, 2, ..., K\})$ when it is ready to transmit. If γ_{d2d} is the SINR at the D2D receiver associated with $\phi_{d2d,j}$, we can write it as $\gamma_{d2d} = \frac{P_{d2d,j}}{I_P + I_{d2d} + \sigma_n^2}$, where $P_{d2d,j}$ is the received power from $\phi_{d2d,j}$, I_P is the interference from primary signals within the k-th sub band, I_{d2d} is the interference from other D2D transmissions, and σ_n^2 is the noise power.

Coverage occurs if $\gamma_{d2d} > \gamma_T$, where γ_T is a threshold SINR level. Coverage probability $\mathbb{P}_C = \Pr[\gamma_{d2d} > \gamma_T]$ may thus be expressed as

$$\mathbb{P}_C = \tau \Pr\left[\frac{\beta P |h_{d2d}| r_{d2d}^{-\alpha}}{I_P + I_{d2d} + \sigma_n^2} > \gamma_T\right] + (1-\tau) \Pr\left[\frac{\rho_{d2d} |h_{d2d}|}{I_P + I_{d2d} + \sigma_n^2} > \gamma_T\right], \quad (13)$$

where τ is defined in (10). Note that for the multi slot harvesting scheme $\tau = 0$, and the first term of (13) vanishes. After several mathematical manipulations and ignoring the negligible interference from D2D transmitters when a full charge does not occur (for the single slot scheme), we can express $\mathbb{P}_C$ as (14) where the remaining integrals must be performed numerically. However, in order to evaluate (14), the MGFs of I_p and I_{d2d} are needed.

$$\mathbb{P}_C=\int_{r_{d2d}=0}^{d_l}\int_{P=0}^{\frac{\rho_{d2d}r_{d2d}^{\alpha}}{\beta}} e^{\frac{-\sigma_n^2\gamma_T r_{d2d}^{\alpha}}{\beta P}} M_{I_p}(\frac{\gamma_T r_{d2d}^{\alpha}}{\beta P})\frac{P^{k_P-1}e^{-\frac{P}{\theta_P}}}{\Gamma(k_P)\theta_P}\frac{2r_{d2d}}{d_l^2}dPdr_{d2d}+(1-\tau)e^{\frac{-\sigma_n^2\gamma_T}{\rho_{d2d}}}M_{I_p}(\frac{\gamma_T}{\rho_{d2d}})M_{I_{d2d}}(\frac{\gamma_T}{\rho_{d2d}}) \quad (14)$$

The interference from PU network is composed of signals from k-th sub band PU transmitters. Thus, these interfering PU transmitters form a thinned homogeneous Poisson point process with density $C_{k,l}\lambda_{pt}$, where $C_{k,l}$ follows (9), and the interference from a single PU transmitter $\phi_{pt,l}$ is written as $I_{P,l} = \rho_p \hat{r}_{k,l}^{\alpha}|h_{l,r}|g(r_{l,r})$, where $|h_{l,r}|$ and $g(r_{l,r}) = r_{l,r}^{-\alpha}$ are respectively the channel power gain and path loss between the l-th interfering PU transmitter and the receiver associated with $\phi_{d2d,j}$. Thus, making use of Slyvniak's and Campbell's theorems, we can write $M_{I_p}(s) = e^{\left(\int_0^{\infty}\mathbb{E}\left[e^{-s\rho_p\hat{r}_{k,l}^{\alpha}|h_{l,r}|r_{l,r}^{-\alpha}}-1\right]2\pi C_{k,l}\lambda_{pt}r_{l,r}dr_{l,r}\right)}$. After first averaging with respect to $|h_{l,r}|$, performing the integral, and finally averaging with respect to $\hat{r}_{k,l}$ we get

$$M_{I_p}(s) = e^{\left(-\frac{2\pi^2 C_{k,l}\lambda_{p,t}(s\rho_p)^{\frac{2}{\alpha}}}{\alpha sin\left(\frac{2\pi}{\alpha}\right)}\mathbb{E}[\hat{r}_{k,l}^2]\right)} = e^{\left(-\frac{2\pi C_{k,l}(s\rho_p)^{\frac{2}{\alpha}}}{\alpha sin\left(\frac{2\pi}{\alpha}\right)}\right)} \quad (15)$$

We now focus our attention on deriving the MGF of I_{d2d}. I_{d2d} is composed of the interference from other D2D transmitters occupying the k-th sub band. For interference to occur from the jj-th D2D transmitter, it must be ready to transmit, be outside guard regions, and must choose the k-th sub band. As these conditions occur independently from other D2D transmitters within Φ_{d2d}, the interfering D2D transmitters can be approximated by a thinned homogeneous Poisson point process with a density of $\frac{\nu p^* \lambda_{d2d}}{K}$, where $* \in \{ss, ms\}$. Now the interference from the jj-th D2D transmitter can be written as $I_{d2d,jj} = P_{jj}|h_{jj,r}|g(r_{jj,r})$, where $|h_{jj,r}|$ and $g(r_{jj,r}) = r_{jj,r}^{-\alpha}$ are the channel power gain and path loss between the jj-th interfering D2D transmitter and the receiver associated with $\phi_{d2d,j}$, while P_{jj} is the transmit power of the jj-th interfering D2D transmitter. Using a similar method to the derivation of (15), we can write $M_{I_{d2d}}$ as

$$M_{I_{d2d}} = e^{\left(-\frac{2\pi^2\nu p^*\lambda_{d2d}s^{\frac{2}{\alpha}}}{\alpha K sin\left(\frac{2\pi}{\alpha}\right)}\mathbb{E}[P_{jj}^{\frac{2}{\alpha}}]\right)}. \quad (16)$$

The expectation $\mathbb{E}[P_{jj}^{\frac{2}{\alpha}}]$ can be expressed as

$$\mathbb{E}[P_{jj}^{\frac{2}{\alpha}}] = \tau\mathbb{E}[\beta^{\frac{2}{\alpha}}P^{\frac{2}{\alpha}}] + (1-\tau)\mathbb{E}[\rho_{d2d}^{\frac{2}{\alpha}}r_{d2d}^2], \quad (17)$$

where the first and second expectations are respectively with respect to $P|P < \frac{\rho_{d2d}r_{d2d}^{\alpha}}{\beta}$ and r_{d2d}. It should be noted that for the multi slot harvesting scheme $\tau = 0$, and the first term will disappear. Thus, after some mathematical modifications, we obtain

$$\mathbb{E}[P_{jj}^{\frac{2}{\alpha}}] = \int_0^{d_l}\frac{2x(\beta\theta_P)^{\frac{2}{\alpha}}}{\Gamma(k_P)d_l^2}\gamma\left(k_P+\frac{2}{\alpha},\frac{\rho_{d2d}x^{\alpha}}{\beta\theta_P}\right)dx+(1-\tau)\frac{\rho_{d2d}^{\frac{2}{\alpha}}d_l^2}{2} \quad (18)$$

1) Probability of a successful transmission: The final probability of a successful transmission during a given time slot ($\mathbb{P}_{C,Total}$) depends on three factors. First, the D2D transmitter should be in the charged state at the start of the time slot. Second, it should not be inside any guard region. Third, if a transmission occurs, the D2D receiver should be within coverage. Considering all three conditions, we can write

$$\mathbb{P}_{C,Total} = p^*\nu\mathbb{P}_C. \quad (19)$$

VI. Numerical Results

Here we investigate successful transmission probability ($\mathbb{P}_{C,Total}$) of an energy harvesting D2D transmitter. Due to limited space, we consider random sub-band assignment only. However, the basic trends remain true for prioritized sub-band assignment. The parameter values are $K = 10$, $\lambda_{d2d} = 10^{-3}$, $\rho_p = -100$ dBm , $d_g = 10$, $M = 5$, $\beta = 0.5$, $\gamma_T = -30$ dBm.

Fig. 2 plots $\mathbb{P}_{C,Total}$ vs. the D2D receiver sensitivity ρ_{d2d}. While $\mathbb{P}_{C,Total}$ increases and keeps constant with ρ_{d2d} for single slot (SS) harvesting, the trend is drastically different for multi slot (MS) harvesting where $\mathbb{P}_{C,Total}$ initially increases and then drops sharply. The initial increase in $\mathbb{P}_{C,Total}$ is due to the increase of $\mathbb{P}_C$ because the desired signal power increases. For SS harvesting, further increasing ρ_{d2d} is counter productive because the probability of acquiring the increased energy is low. However, for MS harvesting, increasing ρ_{d2d} significantly reduces p^{ms} as this scheme always ensures that the required power is harvested before a transmission. Moreover, it is interesting to note that while reducing the primary receiver density increases $\mathbb{P}_{C,Total}$ for SS harvesting, the trend is different for MS harvesting. While reducing λ_{pr} increases $\mathbb{P}_{C,Total}$ for low ρ_{d2d}, the opposite is true for high ρ_{d2d}.

$\mathbb{P}_{C,Total}$ is plotted against the D2D transmitter-receiver distance d_l in Fig. 3. While increasing d_l reduces $\mathbb{P}_{C,Total}$ as expected, the rate of decrease varies significantly for different primary transmitter densities and the energy harvesting scheme. When $\lambda_{pt} = 1 \times 10^{-5}$, the MS harvesting scheme always outperforms the single slot scheme, and the successful transmission probability is consistently low. When $\lambda_{pt} = 1 \times 10^{-4}$, the coverage performance increases, for both energy harvesting schemes. However, while the MS scheme performs better when d_l is lower, the opposite is true for higher d_l. When λ_{pt} is increased further to 1×10^{-5}, the SS scheme performs better under all d_l values. Moreover, the performance of the MS energy harvesting drops drastically as d_l increases. With a higher d_l, a higher power is required for transmission, and with the MS scheme, the D2D transmitter must wait till fully charged before it can transmit. However, because λ_{pt} is high, the powers of the primary transmitters are low due to lower transmitter receiver distances, which means smaller amounts of energy available for harvesting during each time slot. As such, p^{ms} drops significantly, and thus $\mathbb{P}_{C,Total}$ as well.

VII. Conclusion

This paper analyzed the performance of random energy harvesting D2D networks. It considered two energy harvesting

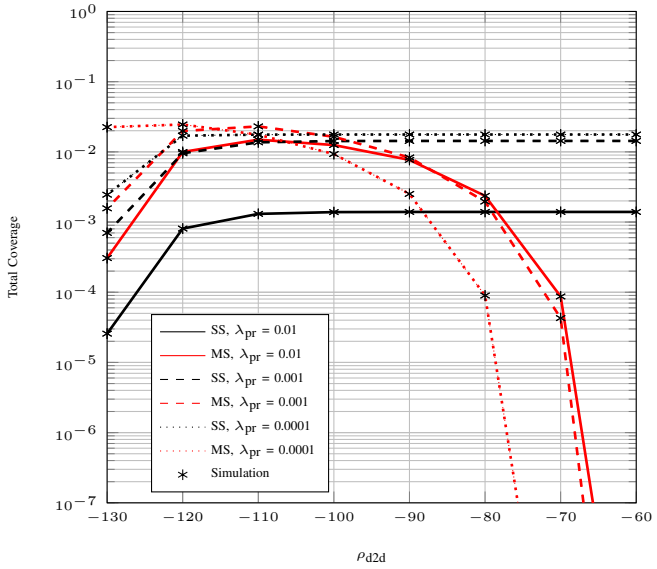

Fig. 2: $\mathbb{P}_{C,Total}$ vs. ρ_{d2d} under random sub-band selection for SS and MS energy harvesting. $d_l = 20$, and $\lambda_{pt} = 10^{-4}$.

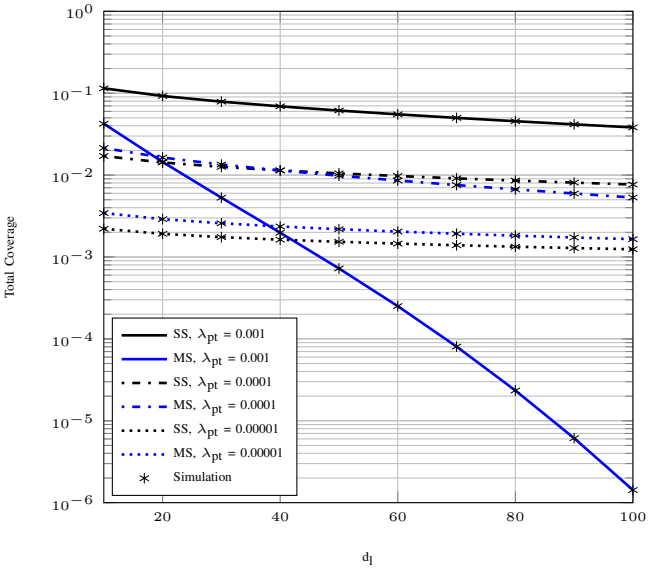

Fig. 3: $\mathbb{P}_{C,Total}$ vs. d_l under random sub-band selection for SS and MS harvesting. $\rho_{d2d} = -100\,\text{dBm}$, and $\lambda_{pr} = 10^{-3}$.

schemes and two channel selection protocols. Random fields of primary transmitters and receivers alongside D2D transmitter-receiver pairs distributed as independent stationary homogeneous Poisson point processes were considered. Several sub-channels for primary transmitter-receiver communication, log-distance path loss and Rayleigh fading were assumed. The MGF and other statistics of the ambient RF power at a D2D transmitter were derived and subsequently approximated by a Gamma distribution. Single slot and multi slot energy harvesting schemes where the latter incorporates temporal correlations were proposed, and the probability of successful transmissions were derived for each using a Markov chain based approach. Moreover, the coverage performance of a D2D link was characterized for 2 sub-band selection protocols. The multi slot harvesting scheme performs better for lower D2D receiver sensitivities and vice-versa. Moreover, an optimum performance occurs for multi slot harvesting when ρ_{d2d} is between $-120\,\text{dBm}$ and $-100\,\text{dBm}$. Furthermore, the primary transmitter and receiver densities significantly affect the total coverage probability of energy harvesting D2D nodes.

REFERENCES

[1] Y. Liu, Y. Zhang, R. Yu, and S. Xie, "Integrated energy and spectrum harvesting for 5G wireless communications," *IEEE Netw.*, vol. 29, no. 3, pp. 75–81, May 2015.

[2] A. Sakr and E. Hossain, "Cognitive and energy harvesting-based D2D communication in cellular networks: Stochastic geometry modeling and analysis," *IEEE Trans. Commun.*, vol. 63, no. 5, pp. 1867–1880, May 2015.

[3] S. Atapattu and J. Evans, "Optimal energy harvesting protocols for wireless relay networks," *IEEE Trans. Wireless Commun.*, vol. 15, no. 8, pp. 5789–5803, Aug 2016.

[4] T. C. Hsu, Y. W. P. Hong, and T. Y. Wang, "Optimized random deployment of energy harvesting sensors for field reconstruction in analog and digital forwarding systems," *IEEE Trans. Signal Process.*, vol. 63, no. 19, pp. 5194–5209, Oct 2015.

[5] S. Jangsher, H. Zhou, V. O. K. Li, and K. C. Leung, "Joint allocation of resource blocks, power, and energy-harvesting relays in cellular networks," *IEEE J. Sel. Areas Commun.*, vol. 33, no. 3, pp. 482–495, March 2015.

[6] S. Lee, R. Zhang, and K. Huang, "Opportunistic wireless energy harvesting in cognitive radio networks," *IEEE Trans. Wireless Commun.*, vol. 12, no. 9, pp. 4788–4799, September 2013.

[7] K. Huang, M. Kountouris, and V. O. K. Li, "Renewable powered cellular networks: Energy field modeling and network coverage," *IEEE Transactions on Wireless Communications*, vol. 14, no. 8, pp. 4234–4247, Aug 2015.

[8] H. S. Dhillon, Y. Li, P. Nuggehalli, Z. Pi, and J. G. Andrews, "Fundamentals of heterogeneous cellular networks with energy harvesting," *IEEE Trans. Wireless Commun.*, vol. 13, no. 5, pp. 2782–2797, May 2014.

[9] J. Ding, L. Jiang, and C. He, "Dynamic spectrum allocation for energy harvesting-based underlaying D2D communication," in *Proc. IEEE VTC*, May 2016, pp. 1–5.

[10] S. Gupta, R. Zhang, and L. Hanzo, "Energy harvesting aided device-to-device communication underlaying the cellular downlink," *IEEE Access*, vol. PP, no. 99, pp. 1–1, 2016.

[11] A. Rabbachin, T. Q. S. Quek, H. Shin, and M. Z. Win, "Cognitive network interference," *IEEE J. Sel. Areas Commun.*, vol. 29, no. 2, pp. 480–493, Feb. 2011.

[12] Z. Chen, C.-X. Wang, X. Hong, J. Thompson, S. Vorobyov, X. Ge, H. Xiao, and F. Zhao, "Aggregate interference modeling in cognitive radio networks with power and contention control," *IEEE Trans. Commun.*, vol. 60, no. 2, pp. 456–468, Feb. 2012.

[13] S. Kusaladharma and C. Tellambura, "On approximating the cognitive radio aggregate interference," *IEEE Wireless Commun. Lett.*, vol. 2, no. 1, pp. 58–61, 2013.

[14] H. Dhillon, R. Ganti, F. Baccelli, and J. Andrews, "Modeling and analysis of k-tier downlink heterogeneous cellular networks," *IEEE J. Sel. Areas Commun.*, vol. 30, no. 3, pp. 550–560, April 2012.

[15] J. F. Kingman, *Poisson Processes*. Oxford University Press, 1993.

[16] A. Goldsmith, *Wireless Communications*. Cambridge University Press, 2005.

[17] A. Molisch, *Wireless Communications*. Wiley-IEEE Press, 2011.

[18] S. Kusaladharma, P. Herath, and C. Tellambura, "Impact of transmit power control on aggregate interference in underlay cognitive radio networks," in *Proc. IEEE ICC*, June 2014, pp. 1–6.

[19] C.-H. Lee and C.-Y. Shih, "Coverage analysis of cognitive femtocell networks," *IEEE Wireless Commun. Lett.*, vol. 3, no. 2, pp. 177–180, April 2014.

[20] S. Kusaladharma and C. Tellambura, "Aggregate interference analysis for underlay cognitive radio networks," *IEEE Wireless Commun. Lett.*, vol. 1, no. 6, pp. 641–644, 2012.

[21] J. Ferenc and Z. Neda, "On the size distribution of poisson voronoi cells," *Phisica A: Statistical Mechanics and its Applications*, vol. 385, no. 2, pp. 518–526, Nov 2007.